**Master's Thesis of Science in Agricultural Biotechnology**

# A colorimetric assay with bi-functional AuNP based on aptamer: On-site detection of *Escherichia coli* O157:H7 in coconut water

## 식품 내 병원성 대장균 O157:H7의 검출을 위한 압타머 기반의 이중기능링커 개발 및 금 나노입자 응집 기반 비색 어세이 개발

**February, 2023**

**The Graduate School**
**Seoul National University**
**Department of Agricultural Biotechnology**

**Min Gyu Lee**

# A colorimetric assay with bi-functional AuNP based on aptamer: On-site detection of *Escherichia coli* O157:H7 in coconut water

Advisor: Young Jin Choi

**Submitting a Master's Thesis of Science in Agricultural Biotechnology**

**February, 2023**

**The Graduate School**
**Seoul National University**
Department of Agricultural Biotechnology

**Min Gyu Lee**

**Confirming the master's thesis written by Mingyu Lee**

**February, 2023**

| | |
|---|---|
| Chair | Ki Won Lee (Seal) |
| Vice Chair | Young Jin Choi (Seal) |
| Examiner | Ju-Hoon Lee (Seal) |

# ABSTRACT

In this study, we developed a colorimetric assay with bi-functional gold nanoparticle (AuNP) based on aptamer for sensitive detection of *Escherichia coli* O157:H7 using the aggregation of AuNP linked with a complementary DNA aptamer specific to *E. coli* O157:H7 aptamer. AuNP was used as a colorimetric linker and probe, respectively, and *E. coli* O157:H7 aptamer and its complementary DNA sequences were modified on each AuNP surface. AuNP labeled with *E. coli* O157:H7 aptamer was used as a bi-functional linker (BL) in a colorimetric competitive assay. Colorimetric assay with BL based on aptamer detected target bacteria by sequential competitive binding between colorimetric probes, which are AuNP having complementary sequences of *E. coli* O157:H7 (AA, Aggregation Assistant) and *E. coli* O157:H7 aptamer. In addition, under optimized conditions by main testing parameters, the assay exhibited a detection range of $10^1$ to $10^6$ CFU/400 μL and a detection limit of 57 ± 0.5 CFU/400 μL. In addition, the developed colorimetric assay with BL based on aptamer was excellently evaluated as an on/off detection system in coconut water, a real matrix. Thus, the proposed colorimetric competitive assay with BL based on aptamer can be a proper on-site detection method of foodborne pathogens. In addition, this study provides the basis for research into developing different colorimetric assay with

aptamer for pathogen analysis in real matrices.

This colorimetric assay with BL based on aptamer functions by driving the system between two competitive interaction dynamics: A) affinity between the aptamer sequence and the target, and B) affinity between the aptamer and the its complementary DNA aptamer.

**Keywords:** colorimetric assay, aptamers, bi-functionable linker, aggregation assistant, *E. coli* 0157:H7, real matrix

**Student Number:** 2021-20519

# CONTENTS

# LIST OF FIGURES

# I. INTRODUCTION

*E. coli* O157:H7 is a gram-negative, rod-shaped, facultative aerobic, and motile bacteria. It is one of the major causes of foodborne illnesses including diarrhea, fever, and death if left undiagnosed and untreated. Severe cases can result in chronic arthritis, brain and nerve damage, and hemolytic uremic syndrome (HUS), which can lead to kidney failure (Chase-Topping et al., 2008; Scheiring et al., 2008). Each year, more than 2 million cases of acute illness worldwide are attributed to *E. coli* O157:H7 (Chekabab et al., 2013). To adequately respond to this disease and its spread, effective monitoring or detection of foodborne pathogens is required.

Various techniques have been developed to appropriately deal with foodborne illness. Traditional detection methods such as polymerase chain reaction (PCR) (Chapman, 2000; Godambe et al., 2017; Holland et al., 2000; Liu et al., 2018), colony-based detection (Deisingh & Thompson, 2004; Saxena et al., 2015), and enzyme-linked immunosorbent assay (ELISA) (Shih et al., 2015) are very accurate and provide high reproducibility, and colony-based detection is somewhat inexpensive for foodborne pathogen detection. Despite their advantages, there are some limits to rapid primary screening detection in the field right after the foodborne illness outbreak because of time-consuming and required manpower or equipment. On-site detection is critical

because one of the key components to combatting bacterial foodborne illnesses is to detect these microbes prior to human infection. For on-site detection, assay must be able to be easily used by layperson without laboratory-level equipment at the point-of-contamination, often in nonideal environments, and accuracy that can quickly detect the target foodborne bacteria.

Recently, several aptasensor using AuNP that acts as signal transducer element of the biosensor (Bhardwaj et al., 2017; Castle et al., 2021; Zhang et al., 2011). The application of aptamer modified AuNP for the highly selective colorimetric detection has been conducted by signaling the presence of target molecules in solution through red to purple color change. However, most of the AuNP-based aptasensors to date have been developed to detect proteins and small molecules (Alsager et al., 2018; Lee et al., 2019), and research on bacteria has been rare and the detection limit has not been useful for on-site detection (Evtugyn, 2016; Rotariu et al., 2016).

In this work, colorimetric detection assay with bi-functional linker (BL) based on aptamer and gold nanoparticle (AuNP) was developed. Until now, bi-functional linker is capped mostly by antibody for certain protein target. Aptamer is comparable to monoclonal antibody in terms of binding affinity, but offers additional decisive advantages. The aptamer is an artificial DNA/RNA-based receptors originated from SELEX (systematic evolution of

ligands by exponential enrichment) (Hong & Sooter, 2015; Mondal et al., 2015; Moon et al., 2015). It can interact with specific proteins and exhibit binding affinities for target bacteria, enzymes, and specific proteins (Ruscito & DeRosa, 2016; Ruscito et al., 2016; Tabarzad & Jafari, 2016; Templier et al., 2016). Aptamer possess advantages of excellent temperature and pH stability, simple chemical synthesis, high productivity, affinity, and the ability to be easily labeled with reporters (Bayat et al., 2018; Berens et al., 2015; Szostak, 1992). This assay generates a visible signal with aggregates of AuNP synthesized by aptamer. To provide clear visible detection to the naked eye, AuNP was used and the aptamer of the *E. coli* O157:H7 target was synthesized into AuNP, this was used as BL, and the AuNP synthesized with the aptamer of the complementary sequence was used as aggregation assistant (AA). The reddish AuNP dispersed in the solution would be aggregated due to the combination of BL and, and maximum aggregation occurs in a specific BL area (The range of linker concentration exhibiting visual color change, REVC) where the optimal quantitative correlation is carried out by forming large-scale aggregates. When a target substance is added to this assay, a change occurs in the existing quantitative correlation between BL and AA. In other words, based on competitive affinity, BL binds to the target rather than AA, and thus the quantitative correlation between BL and AA, which previously achieved maximum aggregation, collapses. Thus, the REVC region appears in a higher

BL region than control line.

In this study, we have developed the colorimetric assay with BL based on aptamer to detect foodborne bacteria, *E. coli* O157:H7. Based on the salt-induced aggregation of AuNP and complementary sequence, *E. coli* O157:H7 in coconut water was specifically detected. For on-site detection, we presented a bacterial detection method for liquid solution, which was validated by applying the method to coconut water.

# II. MATERIALS AND METHODS

## 2.1. Materials

The bacterial strain used in the assay was *E. coli* O157:H7 (ATCC 43890), *E. coli* K12 (10798), *Staphylococcus aureus* (25923), and *Salmonella* Enteritidis (14544). Chloroauric acid was purchased from Sigma Aldrich (St. Louis, MO, USA). Tri-sodium citrate was purchased from Yakuri Pure Chemicals Co., Ltd (Kyoto, Japan). The *E. coli* O157:H7, 5`-TGG TCG TGG TGA GGT GCG TGT ATG GGT GGT GGA TGA GTG TGT GGC-thiol-3` (Yu et al., 2018) and its complementary DNA aptamer, 5`-GCC ACA CAC TCA TCC ACC ACC CAT ACA CGC ACC TCA CCA CGA CCA-thiol-3`, was synthesized from bioneer, Ltd (Seoul, Korea). 1-mM tetrachloroaurate and 4-(2-hydroxyethyl)-1-piperazineëthanesulfonic acid (HEPES) was purchased from Thermo Fisher Scientific (Waltham, MA, USA). Coconut water was purchased from Malee juice & malee coco, Ltd (Bangkok, Thailand).

## 2.2. Instrumentation

Absorbance measurements were performed on a UV-1700 spectrophotometer (Shimadzu, Kyoto, Japan). The pH values of all buffer solutions were determined using the Professional Meter PP-15 (Satorious,

Göttingen, Germany). Particle sizes and distributions were determined by dynamic light scattering (DLS) with a Zetasizer Nano-ZS 90 (Malvern, Worcestershire, UK). Transmission electron microscopic (TEM) images were obtained using a LIBRA 120 transmission electron microscope (Karl Zeiss, Oberkochen, Germany). An autoclave MR-AC 60 (Mirae science, Gunpo, Korea) was used to sterilize samples.

## 2.3. Culturing of Bacteria

All bacteria was inoculated into luria-bertani (LB) broth. A single colony was picked from the plate, inoculated into 5 mL of Tryptic soy broth medium, and maintained overnight at 37°C in a shaking incubator. The cultures containing bacteria were centrifuged at 4,000 g for 20 minutes. The pallet was then dispersed in HEPES buffer (10 mM, pH 7.4). Serial dilutions of the cultures were made in HEPES and 100 μL of diluted suspension was inoculated onto agar plates for counting. The final suspensions contained a *E. coli* O157:H7 concentration of $6.3 \times 10^8$ CFU/mL. All other bacteria used as controls were cultured in the same manner.

## 2.4. Preparation of gold nanoparticles (AuNP)

Gold nanoparticles (AuNP) 13.0 ± 0.5 nm in diameter were

synthesised by reducing tetrachloroaurate with trisodium citrate, a commonly used method (Hauser & Lynn, 1940). Briefly, 150 mL of sodium citrate solution (2.2 mM) was brought to boiling. Once boiling had begun, 1 mL of chloroauric acid (HAuCl4) solution (25 mM) was added to the boiling solution. When the colour of the solution had changed to soft pink, the solution was cooled to 90 °C in a water bath, and the cooled solution was used as a seed solution for the growth process. The particle sizes of the AuNP had an ultraviolet-visible (UV-Vis) spectrum peak at approximately 520 nm, which corresponds to an average diameter of 13 nm.

## 2.5. Modification of AuNP with aptamer

To functionalize and modify of AuNP with aptamer, we conjugated thiolated DNA to AuNP by adjusting the pH, which is a partial modification of the technique (Liu & Liu, 2017, 2019). Briefly, TCEP (20 mM) was mixed in equal amounts with the thiolated aptamer to cleave disulfide bonds and generate free-terminal thiols in DNA (Zhang et al., 2013). 13 nm AuNPs are mixed with thiolated DNA in a washed vial or microcentrifuge tube. By using a 100:1 ratio (for adsorption capacity) the system should perform similarly. After a short incubation period, a final aliquot of 10 mM sodium citrate buffer was quickly added (500 mM sodium citrate stock solution, pH 3.0). After 3

minutes, samples were centrifuged to remove unbound free DNA and redispersed in pH 7 buffer for use. Here, the role of acid is also to overcome the kinetic barrier of DNA binding. Once the AuNP/thiol bond is formed, it is thermodynamically very stable. After this, through the absorbance measurements, the absorbance at 520 nm was unified to 4.0 by redispersing with 50 mM Tris-HCl buffer. Through this process, BL AuNP conjugated with *E. coli* O157:H7 aptamer and AA AuNP conjugated with cDNA aptamer were prepared.

## 2.6. Optimization of NaCl concentrations

To determine the optimal NaCl concentration, the concentrations were set at 0, 10, 20, 40, 80, 100, 150, 200, 300, and 400 nM. After combining 200 μL of BL or AA AuNP with 100 μL of HEPES buffer (10 mM, pH 7.4) for 30 minutes. Then, 50 μL of NaCl per concentration was added and incubated for 10 minutes. Transmission electron microscope (TEM) images revealed that the absorbance reflected the degree of aggregation and sedimentation of AuNP in the $A_{620}/A_{520}$ ratio.

## 2.7. Detection of *E. coli* O157:H7 in samples

*E. coli* O157:H7 aptamer with AuNP as the BL and cDNA aptamer

with AuNP as AA were used in this assay. Briefily, the assay was performed in a total reaction volume of 400 μL containing 300 μL of BL and AA mixture and 100 μL of a test sample. First, 100 μL of test sample was mixed with 100 and 120 μL of BL. After sufficient reaction time (> 60 minutes) without agitation, 200 and 180 μL of AA was added to the mixture and the samples were agitated for 60 minutes. Color changes in the reaction were monitored to determine quantitative correlations between samples, BL, and AA. In colorimetric assays with BL based on aptamer, it is important to determine the REVC of AuNP. Therefore, before applying the colorimetric assays with BL based on aptamer for the detection of *E. coli* O157:H7, we determined REVC of the AuNP used in this study. To find REVC, we performed assays in HEPES with different amounts of BL and AA (20&280–280&20 μL). According to REVC confirmation, these amounts were considered the most effective for rapid on-site detection of *E. coli* O157:H7 in samples because they provide a simple color change.

## 2.8. Verification of the selectivity of the detection method

To determine the selectivity of a colorimetric assay using aptamer-based BL, a protocol was performed using 4 strains of bacteria at a concentration of $10^4$ CFU/400 μL: *E. coli* O157:H7 (ATCC 43890), *E. coli*

K12 (ATCC 10798), *Staphylococcus aureus* (ATCC 25923), and *S.* Enteritidis (ATCC 14544). BL was added to five solutions: *E. coli* O157:H7, *E. coli* K12, *Staphylococcus aureus*, *S.* Enteritidis, and negative control (HEPES). After 60 minutes, AA was added to each sample. The peak absorbance of the mixture was measured with a UV-Vis spectrophotometer 60 minutes after the addition of AA, and the difference in absorbance between the two concentrations was calculated.

## 2.9. Statistical analysis

The data represent an average of at least three independent experiments or measurements, and the results are expressed as mean ± standard deviation (SD).

# III. RESULTS AND DISCUSSION

## 3.1. Overall detection procedures

In this study, an on-site colorimetric detection method was proposed to detect *E. coli* O157:H7 in food easily and rapidly.The proposed detection method should consist of two sequential steps: (1) the reaction of BL and the sample, which is the target recognition step, and (2) the addition of AA following the expiration of the reaction time, 60 minutes, which is the signal indication step. The diagrams in Figure 1 and 2 shows the colorimetric assay with BL based on aptamer. First, *E. coli* O157:H7 targeting aptamers and aptamers with complementary sequences were synthesized into AuNP, respectively, and these were designated as BL and AA. The BL is a mediator of aggregation that can form aggregates with both targets and AA. With regard to AA, AA is designed to bind to BL but not the target due to the complementary sequence of AA. As can be seen, when each AuNP existed independently, it was separated by maintaining a distance respectively 50 to 200 nm. However when BL and AA were mixed, it was confirmed that they were combined through the binding of their complementary sequences (Fig. 3). This confirmed that the second function of the bifunctional linker, the binding between AuNP, has been attained.

The vast majority of the system through which BL and AA are synthesized in manner consists of particle aggregation and precipitation reactions. The combination of BL and AA aggregates the reddish AuNP dispersed within the solution. In the specific BL region where the optimal quantitive correlation is formed with AA, maximum aggregation of AuNP occurs, resulting in large-scale aggregates. As can be seen, these large-scale aggregates of AuNP settle out rapidly over time, and specific BL regions appear as sunken regions. We subtitles this region REVC. Based on REVC, the system is divided into three areas: A section where precipitation does not occur because the number of BL is insufficient to cause large-scale aggregation, the revc section where large-scale aggregates are formed and precipitated as a result of the optimal quantitative correlation between BL and AA. Finally, the quantitative correlation is reversed due to excessive linkers, and rather, it is the section where aggregation did not occur.

However, this aggregation zone, REVC, shifts in accordance with the change in the quantitative correlation when the target material is added. As the previously used BL binds to the target, the existing quantitative correlation is broken, and the amount of switched-off BL increases as the concentration of the analyte increases. Eventually, a higher concentration of BL was required for the large-scale aggregation that appeared in the REVC region. Consequently, there is a migration of REVC to regions of higher

concentrations of BL. Therefore, this system can quantitatively detect the analyte by using the difference in REVC between the control line without the analyte and the test line with the analyte.

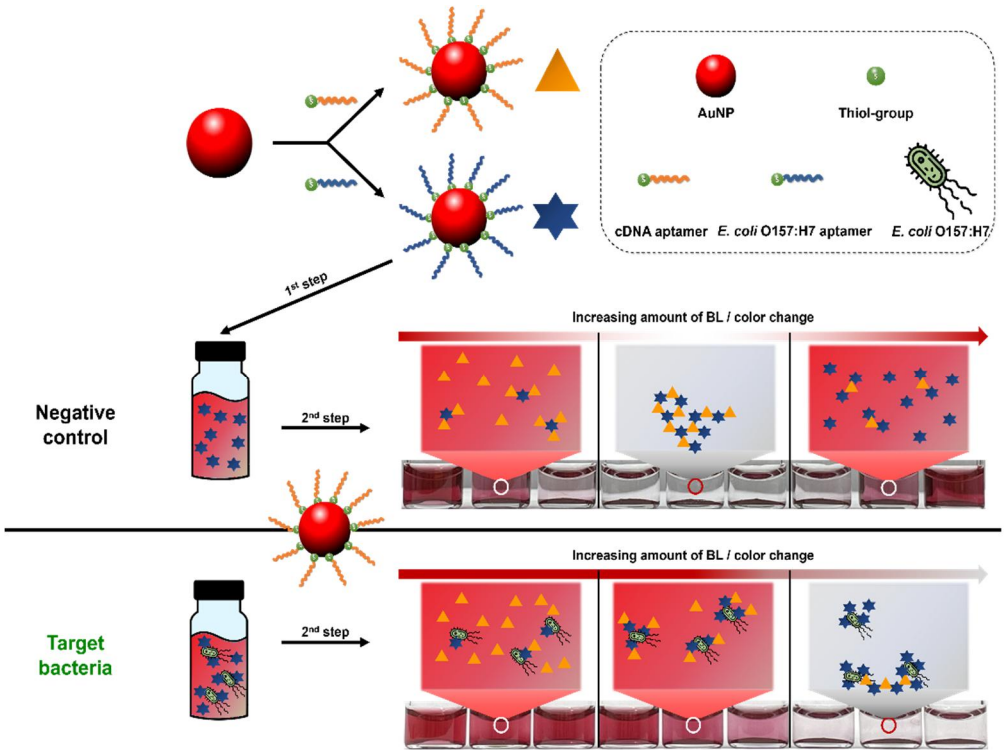


**Figure 1.** Schematic diagram of colorimetric assay with bi-functional linker based on aptamer to detect *E. coli* O157:H7.

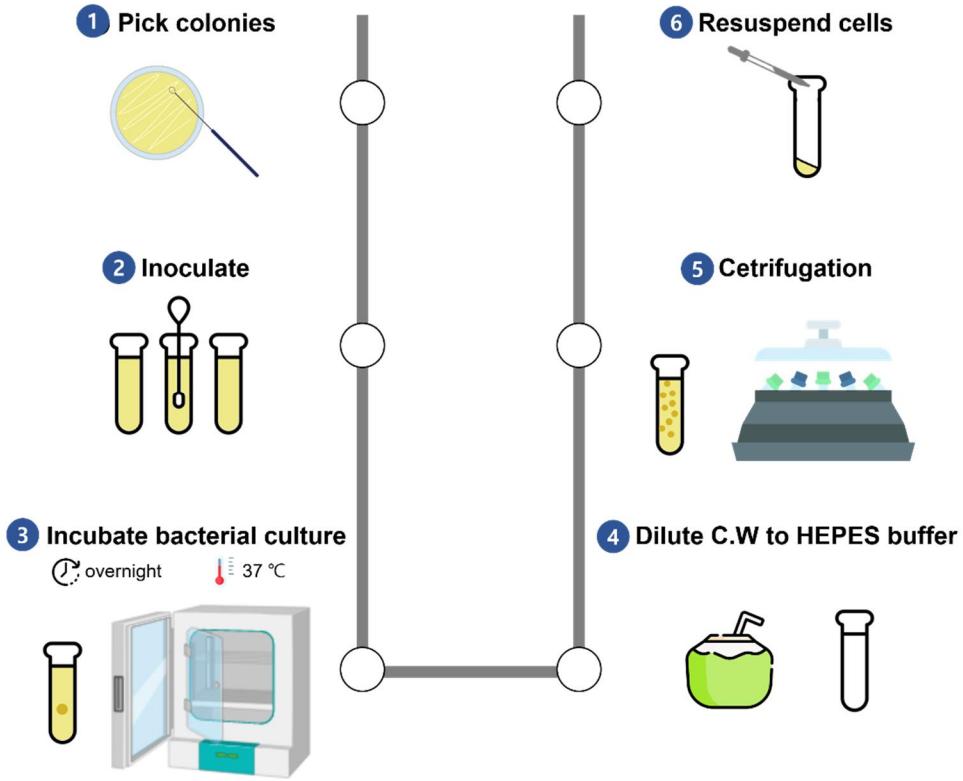


**Figure 2.** Schematic diagram of coconut water extraction process.

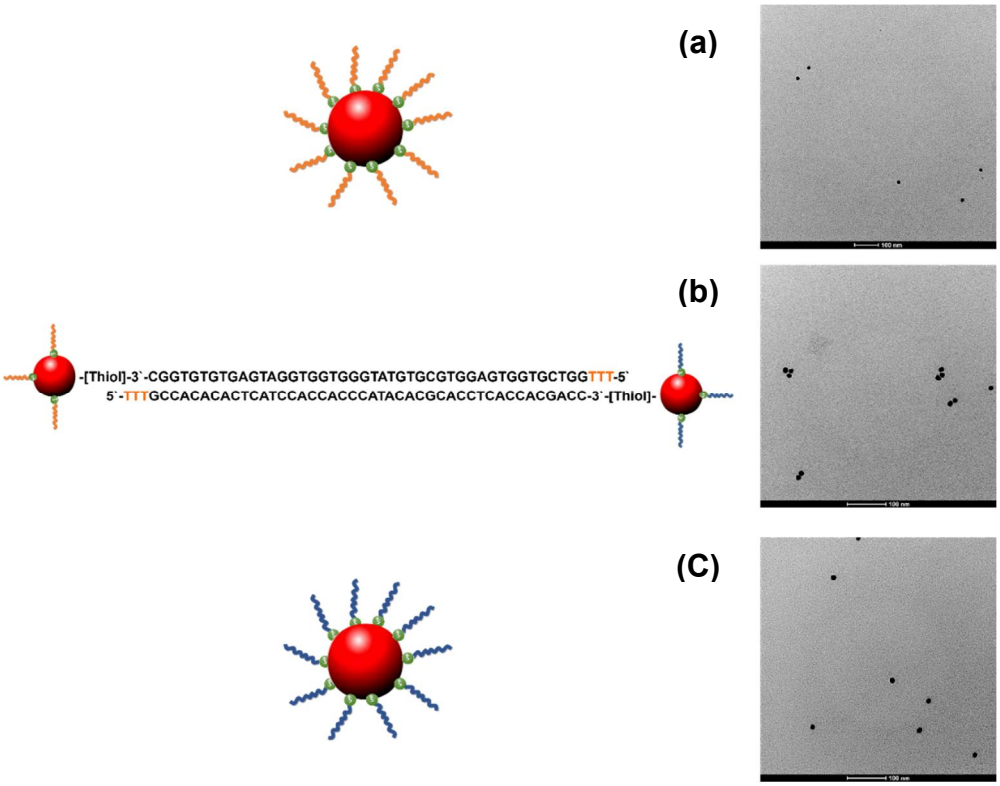


**Figure 3.** The TEM images of AuNP: (a) AA with 150 mM NaCl; (b) AA with 150 mM NaCl + BL with 150 mM NaCl; (c) BL with 150 mM NaCl.

## 3.2. Optimization of NaCl concentrations

AuNP possess strong interparticle van der Waals forces, and citrate-capped AuNP is stabilized only by weak electrostatic repulsion and readily aggregates at slightly higher ionic strengths (Luan et al., 2015; Matsunaga et al., 2019). Consequently, the degree of AuNP aggregation was dependent on the various NaCl concentrations (Fig. 4 and 7).

It is well known that the ultraviolet-visible (UV–Vis) spectrum of AuNP solutions exhibits a strong absorption band in the visible region (500 nm to 600 nm). This is because the spectrum is red-shifted by the aggregation of AuNP. At 620 and 520 nm, the absorbant coefficients are proportional to the amount of dispersed and aggregated AuNP, respectively. Therefore, the degree of aggregation was determined with $A_{620}/A_{520}$ ratio, the ratio of absorbance at these two wavelengths, with NaCl concentrations ranging from 10 to 400 mM (Fig. 5 and 8). In the absence of NaCl, the $A_{620}/A_{520}$ ratio for test solutions was approximately 0.1. NaCl addition to the mixture slightly decreased the absorbance at 520 nm, but there was no shift in the absorbance peak. Concentration had no impact on the neutralized surface charge of AuNP. Saturation concentration was observed from 200 mM NaCl concentration, with NaCl addition to the test solutions at a final NaCl concentration of 200 mM and higher, and the $A_{620}/A_{520}$ ratio of the test solutions increased

significantly to approximately 0.4, so 150 mM concentration was the concentration before saturation, demonstrating a large change (Fig. 6 and 9). Therefore, an appropriate concentration of NaCl was required and a concentration of 120 mM was optimally chosen.

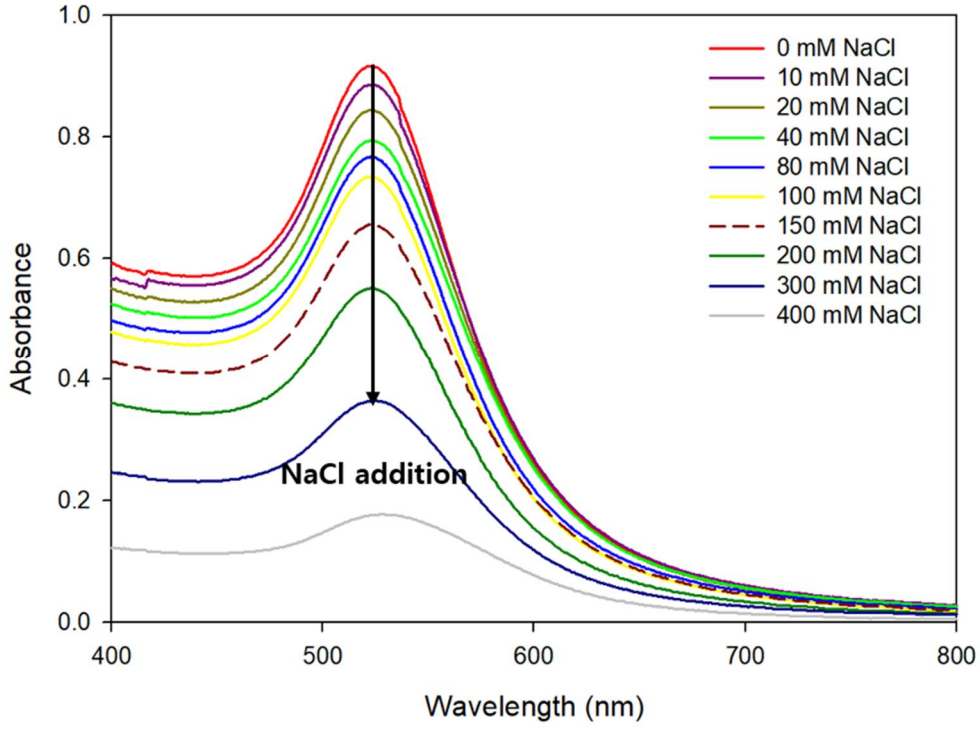


**Figure 4.** The absorbance of BL AuNP according to various NaCl concentrations.

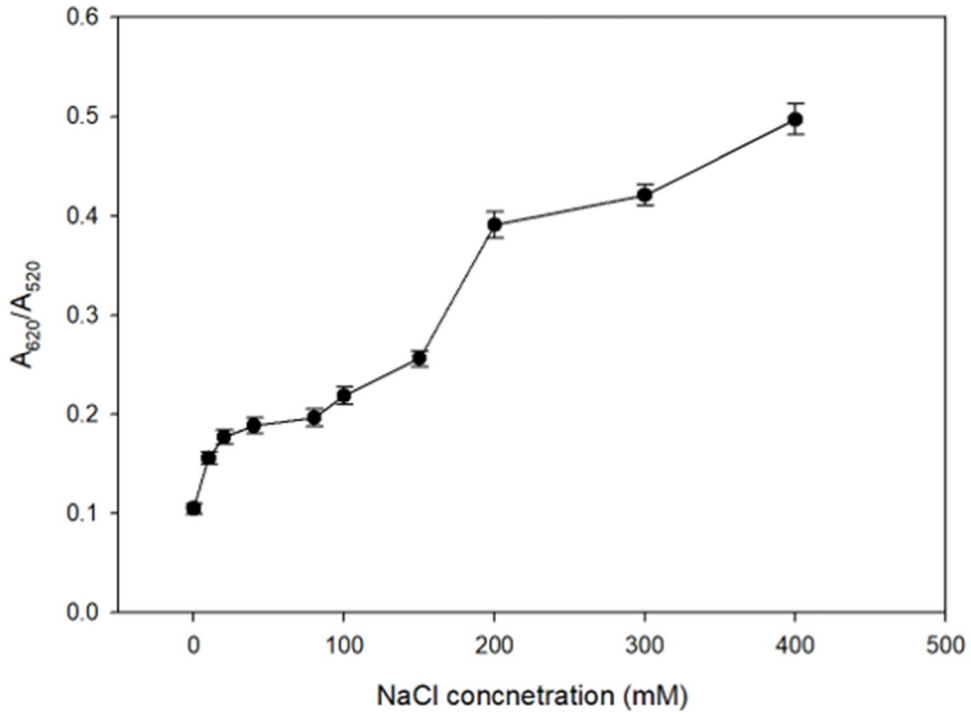


**Figure 5.** The aggregation degree ratio ($A_{620}/A_{520}$) of BL AuNP according to various NaCl concentrations.


**Figure 6.** The color change of BL AuNP according to various NaCl concentrations.

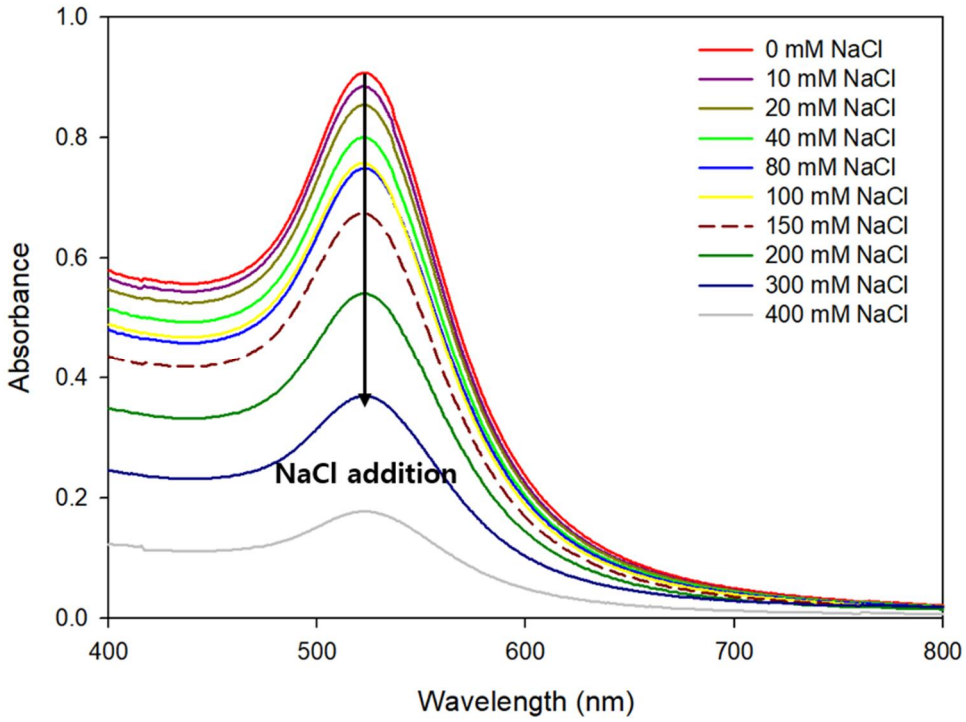


**Figure 7.** The absorbance of AA AuNP according to various NaCl concentrations.

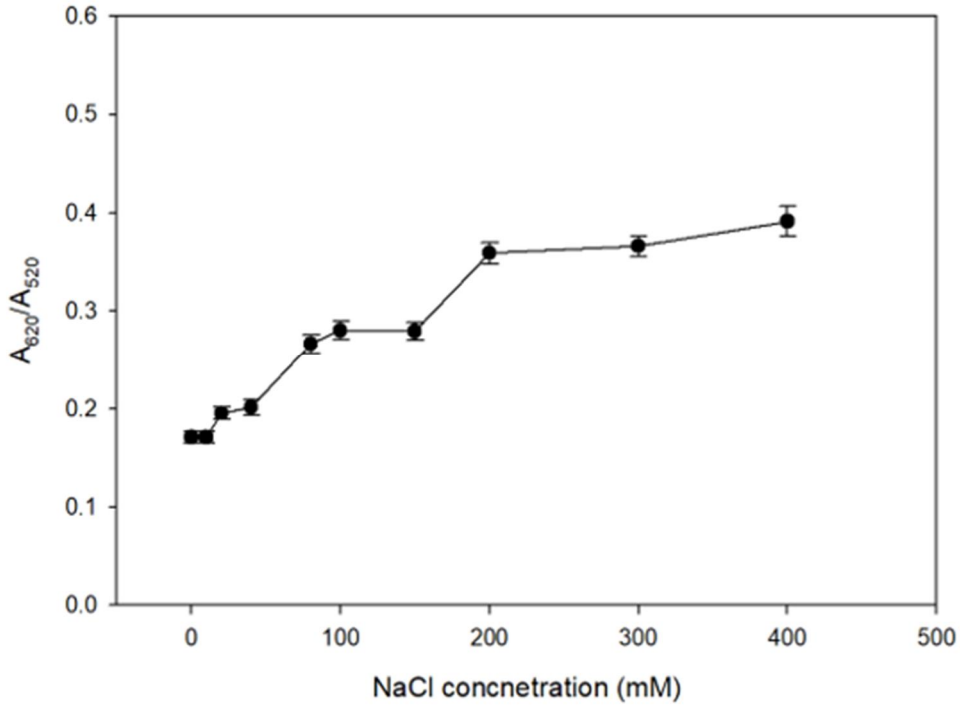


**Figure 8.** The aggregation degree ratio ($A_{620}/A_{520}$) of AA AuNP according to various NaCl concentrations.

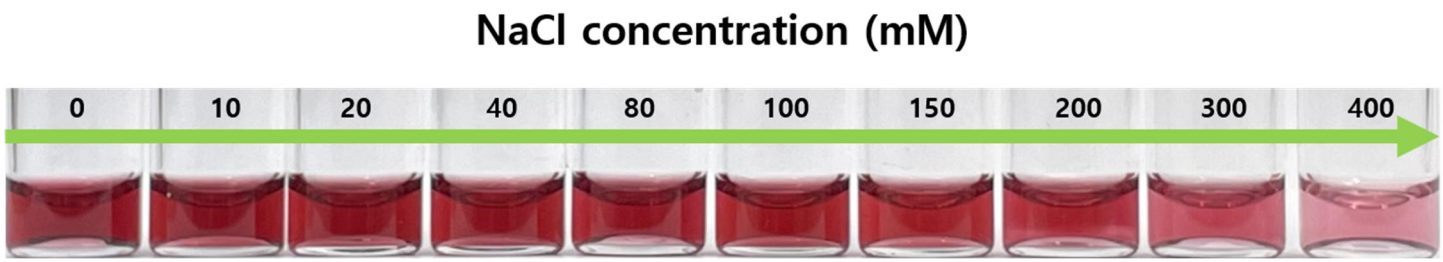


**Figure 9.** The color change of AA AuNP according to various NaCl concentrations

## 3.3. Selectivity of the colorimetric assay

The specificity of the assay was evaluated using a variety of different bacteria, including control samples (just HEPES buffer), *E. coli* K12, *Staphylococcus aureus*, and *S.* Enteritidis to confirm that such color changes are caused by the binding of the aptamer to the target bacteria.

As shown in Figure 10a, only the *E. coli* O157:H7 sample exhibited a significant color change. In addition, the Absorbance at 530 nm of AuNP (BL: 120 μL, AA: 180 μL) in the presence of *E. coli* O157:H7 was 2.16 times that of other bacteria (Fig. 10b).

These results of other bacteria demonstrated that this assay could identify target bacteria with high degree of specificity, whereas other bacteria were unable to differentiate aptamer from AuNP with minimal color change.

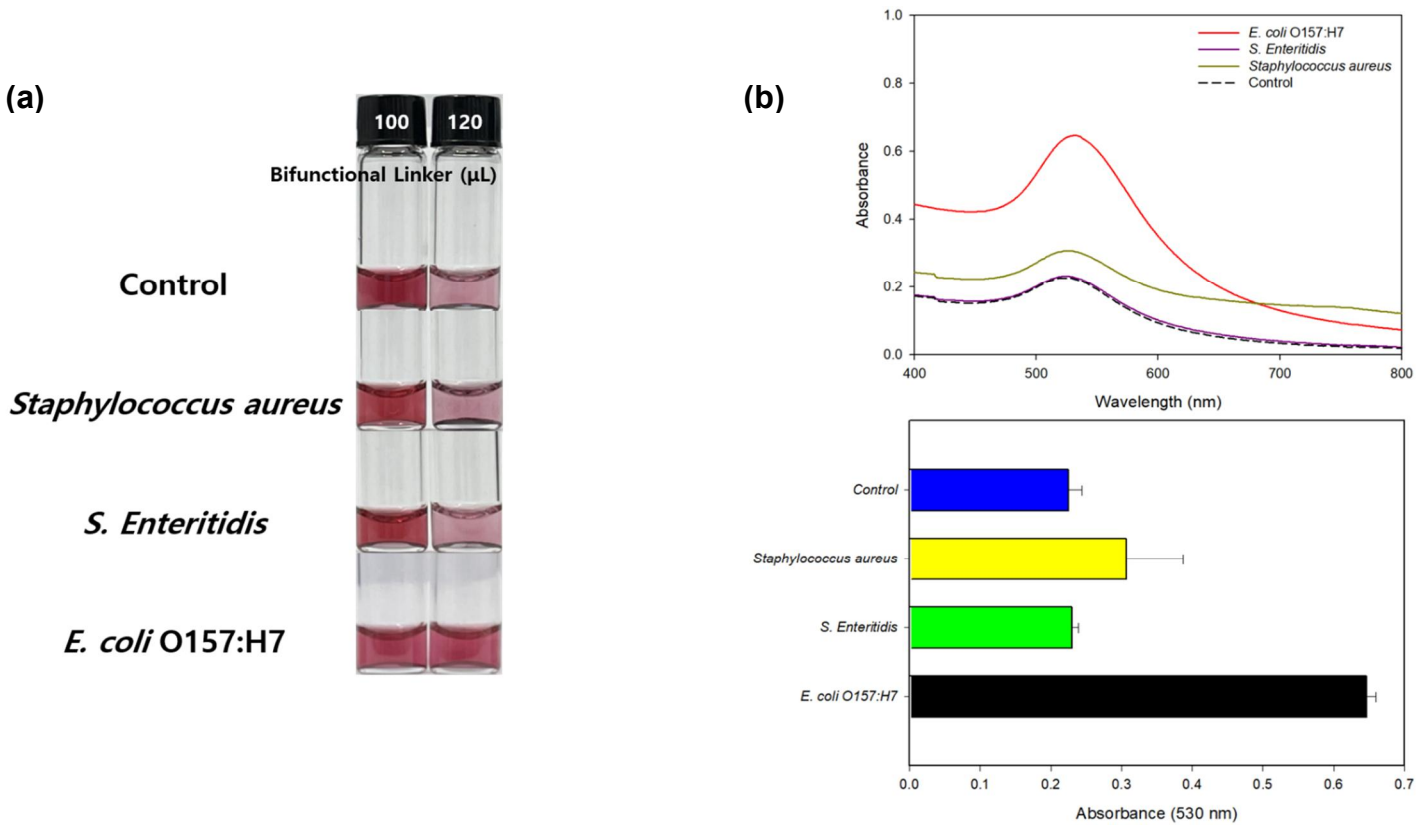


**Figure 10.** Selectivity of colorimetric assay with BL based on aptamer. (a) The color change of AuNP according to various samples. (b) The absorbance of AuNP according to various samples.

## 3.4. The range of REVC

This colorimetric assay with BL based on aptamer used REVC determined based on quantitative correlations between BL, AA, and target. To assess the extent of target-induced shift in REVC, we first had to determine naturally occurring REVC using only BL and AA as controls. Although the amounts of BL and AA were varied, their total amount, AuNP, was fixed to maintain a constant color. Therefore, REVC shift was solely determined by the quantitative correlation between BL, AA and target. BL amounts of 120 to 220 μL in HEPES were selected as the amounts most likely to show REVC (Fig. 11). Since aggregation did not occur at 100 μL and aggregation occurred at 120 μL, it was determined that those amounts were the divergence points of region 1 and REVC. That is, when the target bacteria were introduced, it was considered that the color change due to the change in quantitative correlations at this point was most pronounced, and the experiment was performed at the corresponding detection concentration, so BL amounts of 100, 120, and 140 μL were used to detect *E. coli* O157:H7.

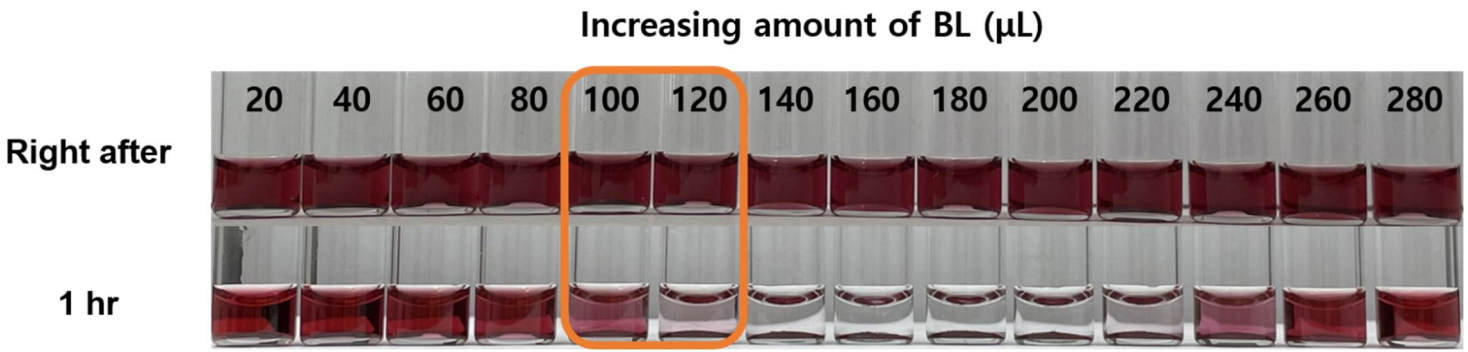


**Figure 11.** The visual signal results of negative control with various BL amount between 20 to 280 µL in HEPES buffer according to agitation time.

## 3.5. Detection of *E. coli* O157:H7 in HEPES buffer

Prior to application on-site, this detection technique should be tuned in terms of the REVC shift generated by *E. coli* O157:H7 that is affected by the amounts/ratios of BL and AA. As shown in Fig. 12, we first calculated the REVC signal of the control (no target). This REVC signal was seen at BL amounts between 120 and 220 μL. At amounts of BL ranging from 160 to 200 μL, a clear precipitate was noticed between BL and AA, but a little color difference (purplish red) was observed at amounts of 120 (low end) and 220 μL (high end). This color variation is primarily attributable to the SPR difference caused by the presence of tiny, unprecipitated BL-AA aggregates. In the presence of *E. coli* O157:H7 ($10^1$ CFU/400 μL), the amount ranges of BL 160 to 220 μL exhibited a right-side REVC shift relative to the control REVC. In the meantime, the amount ranges of BL utilized for the *E. coli* O157:H7 detection were further subdivided to gain a more quantitative and sensitive signal change (such as the REVC shift), and the BL concentration ranges were determined to be 100 and 120 μL (*E. coli* O157:H7, more than $5.7 \times 10^1$ CFU/400 μL). When just BL and AA aggregated in the absence of *E. coli* O157:H7 as a control sample, precipitation occurred at all amounts with the exception of a BL concentration of 80 to 100 (the lowest in this experiment) and 240 to 260 μL (the highest in this experiment). As the amount of *E. coli*

O157:H7 that had been reacted grew, the REVC gradually changed to greater BL amounts. As depicted in Fig. 13 and 14, as the amount of *E. coli* O157:H7 rose from 0 (control samples) to $10^6$ CFU/400 μL, the REVC shift at the low end was clearly evident and the color of sample with BL amounts of 120 μL turned to red. The precipitation region could be distinguished with the naked eye alone, without the use of an instrument. To evaluate and confirm this technique at the indicated BL values, we employed colony-based detection to detect and compare different *E. coli* O157:H7 concentrations (0, $10^1$, $10^2$, $10^4$ CFU/400 μL). Due to these factors, it is considered that this strategy can be useful and applicable in the field.

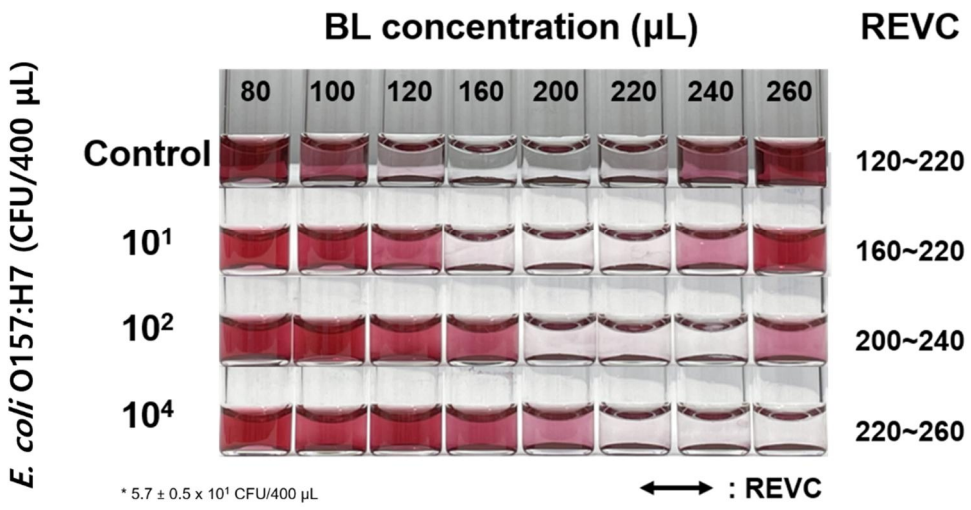


**Figure 12.** Shifting of the REVC in response to the presence of *E. coli* O157:H7 in standard solution (0, $10^1$, $10^2$, $10^4$ CFU/400 μL).

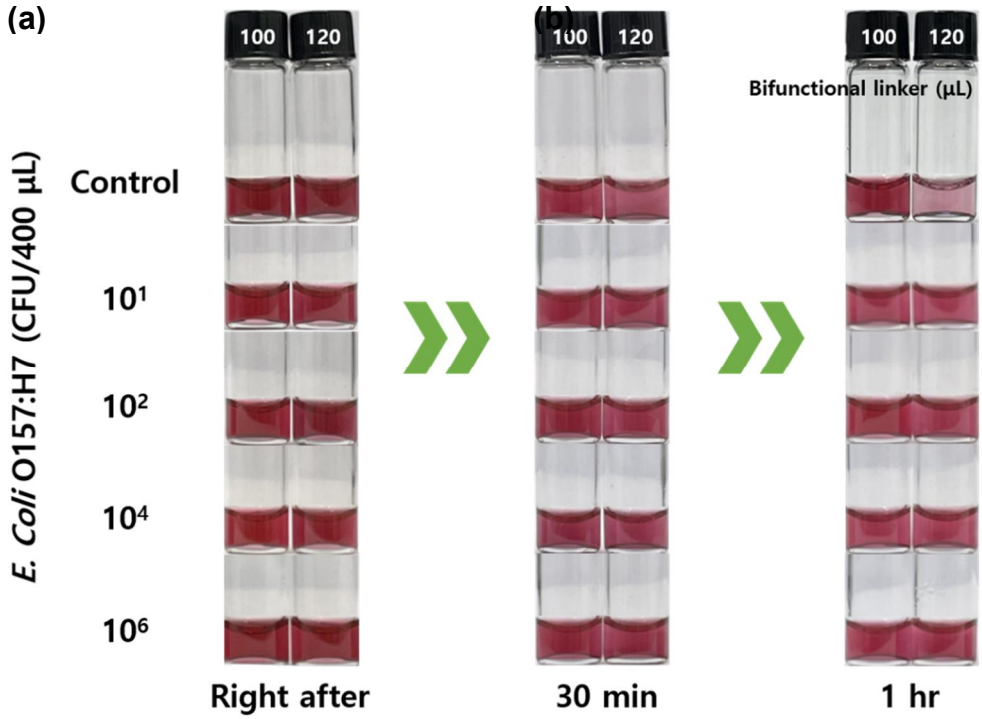


**Figure 13.** Colorimetric assay response towards a range of *E. coli* O157:H7 concentrations (0, $10^1$, $10^2$, $10^4$, $10^6$ CFU/ 400 μL) using the BL-AA according to time.

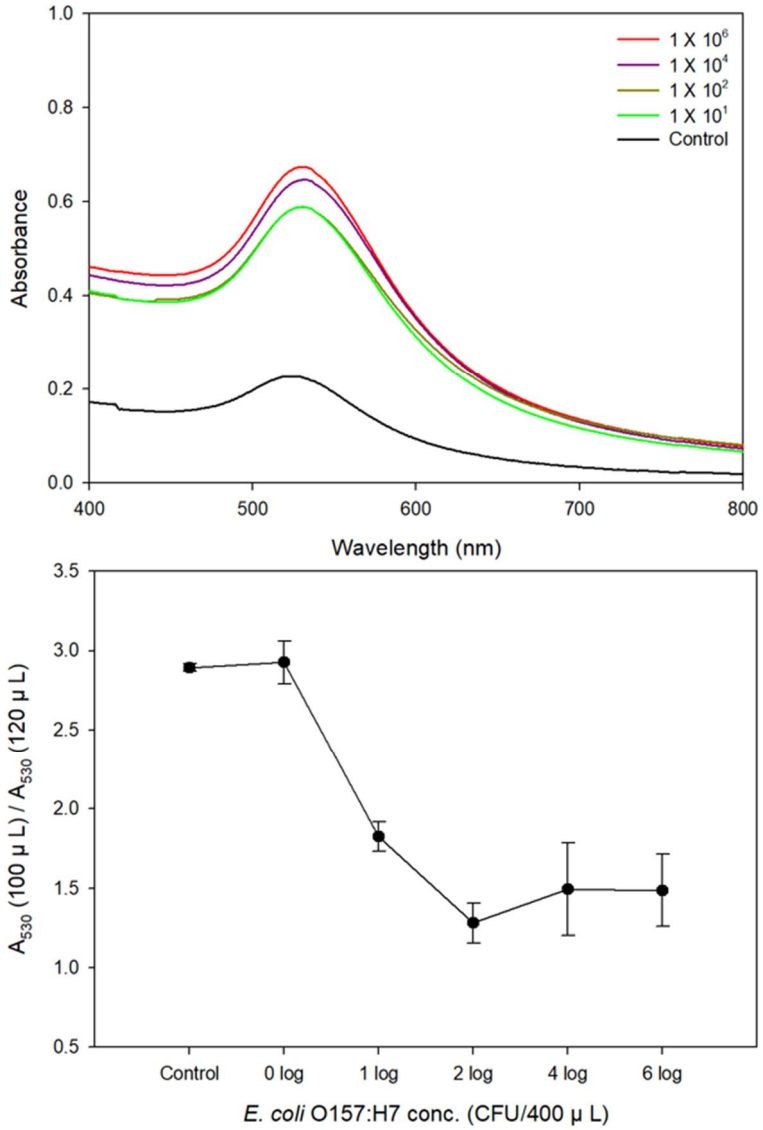


**Figure 14.** UV-vis absorption spectra for colorimetric assay response towards a range of *E. coli* O157:H7 concentrations (0, $10^1$, $10^2$, $10^4$, $10^6$ CFU/ 400 µL) using the 120 µL of BL.

## 3.6. Detection of *E. coli* O157:H7 in coconut water

The detection of pathogens in food is complicated, not only because of the large pH range, but also because numerous nutritional components can interfere with biosensor signals. However, colorimetric assay with BL based on aptamer may establish a base-control for each food sample, ensuring that only the pathogen is responsible for the REVC shift. Pathogens can be detected utilizing the difference in REVC between pathogen-free controls and pathogen-containing controls.

Coconut water were tested with the detection method to determine its applicability to real samples. Coconut water, extracted from the liquid endosperm of young coconuts, is gaining popularity as a natural carbohydrate-electrolyte-rich beverage that may readily inhibit bioassays. However, it must be mildly processed to preserve its qualities and reduce food poisoning risk (Adolf K et al., 2012; Gabriel & Arellano, 2014; Gayán et al., 2020). The coconut water was chosen as a representative food sample for system validation for this reason.

In order to control the concentration of *E. coli* O157:H7, test samples spiked with varying concentrations of target bacteria, *E. coli* O157:H7, ranging from 0 to $10^6$ CFU/ 400 μL were prepared and subjected to analysis. The outcome is exceptionally effective for identifying *E. coli*

O157:H7 on a variety of foods, including coconut water. Comparing control coconut water samples with HEPES buffer, the low end of REVC was 140 μL BL for coconut water and 120 μL BL for HEPES buffer (Figure 11 and 15). In contrast to conventional biosensors, which are limited by the effects of food composition, the colorimetric assay with BL based on aptamer can detect *E. coli* O157:H7 at commercial coconut water processing and distribution sites when a base control is available. In addition, the colorimetric assay with BL based on aptamer utilizes the large-scale aggregation of AuNP to produce color, and it is not impacted by the natural color of coconut water by diluting with HEPES buffer.

In order to test directly at commercial sites, testing procedures must be simple, fast, and straightforward. Therefore, we decreased the BL amounts to 100, 120, and 140 μL in order to qualitatively assess the REVC shift at the low end. Moreover, there are far more aptamers than *E. coli* O157:H7 may react with in the case of a BL-*E. coli* O157:H7 interaction, despite the low *E. coli* O157:H7 concentration. This indicates that the REVC can alter sensitively at low *E. coli* O157:H7 concentrations. Consequently, the chosen BL accounts (100, 120, and 140 μL) ought to provide a REVC shift for the ultrasensitive detection of *E. coli* O157:H7 in coconut water.

The low end of REVC for *E. coli* O157:H7-contaminated samples was different with control sample (Figure 15). Even *E. coli* O157:H7

concentrations as low as $6.3 \times 10^1$ CFU/400 μL were detectable. Frequently, coconut water is cross-contaminated with trace amounts of *E. coli* O157:H7 in contaminated water, but the germs multiply fast at room temperature during shipping or retail display. Therefore, the identification of *E. coli* O157:H7 at low concentrations is crucial.

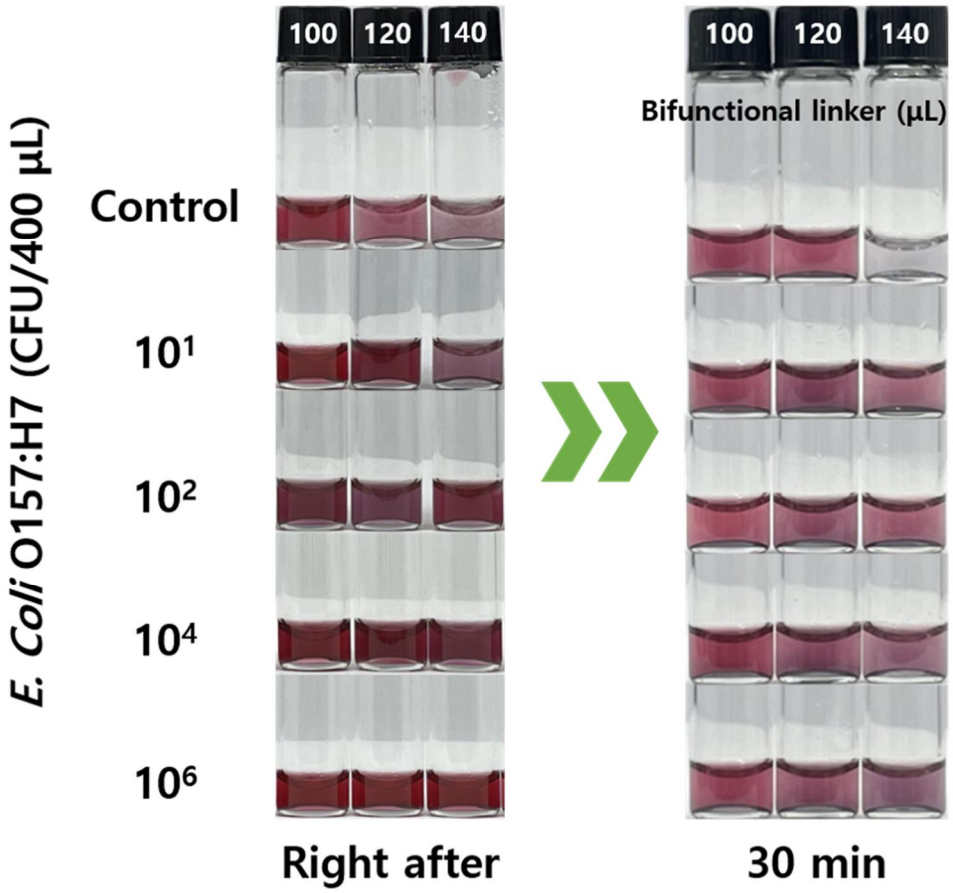


**Figure 15.** Colorimetric assay response towards a range of *E. coli* O157:H7 concentrations (0, $10^1$, $10^2$, $10^4$, $10^6$ CFU/ 400 μL) in coconut water using the BL-AA according to time.

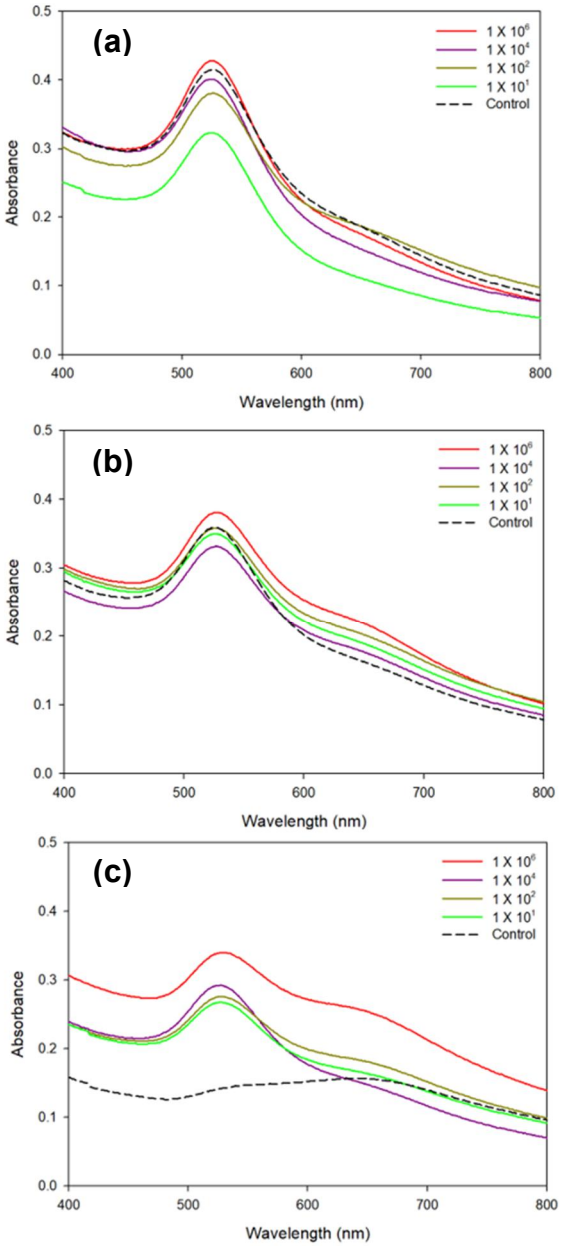


**Figure 16.** UV-vis absorption spectra for colorimetric assay response towards a range of *E. coli* O157:H7 concentrations (0, $10^1$, $10^2$, $10^4$, $10^6$ CFU/ 400 µL) using the (a) 100; (b) 120; (c) 140 µL of BL in coconut water.

# CONCLUSION

*E. coli* O157:H7 detection in coconut water is essential since these items are not sterilized. Even while coconut water may contain a modest concentration ($10^2$–$10^3$ cells per gram) of *E. coli* O157:H7, the bacteria can proliferate rapidly at room temperature, resulting in a severe outbreak. Our colorimetric assay with BL based on aptamer utilizing the large-scale aggregation of AuNP demonstrated excellent potential for sensitive, fast, colorimetric detection of *E. coli* O157:H7 in contaminated coconut water samples, making it commercially applicable. In addition, we developed a simple and rapid method for detecting *E. coli* O157:H7 based on BL-induced AuNP precipitation, as well as a simple method for extracting *E. coli* O157:H7 from food by diluting the stock solution by a factor of half.

To use an assay for multiplexing detection and for use in scaling the system to high sample volumes, additional research is required. Such an assay could be utilized as a practical tool for the on-site analysis of a variety of food items, including raw fruits and vegetables.

Utilizing *E. coli* O157:H7 aptamer and cDNA aptamer as a detector and helper for AuNP aggregation, we have created colorimetric assay with BL based on aptamer that can detect bacteria with the naked eye in a quick and selective manner. This innovative technique is straightforward and can be

utilized for the quick identification of diarrheal illnesses. Nonetheless, the greatest advantage of this assay is its direct detection of entire bacteria without the need for specialist equipment and preparatory steps such as cell lysis. Furthermore, this approach might theoretically be used to detect other bacteria by swapping aptamer.

# REFERENCES


Adolf K, A., Edna D, D., & Rebecca, A. (2012). Potential bacterial health risk posed to consumers of fresh coconut (Cocos nucifera L.) water. *Food and Nutrition Sciences*, *2012*.

Alsager, O. A., Alotaibi, K. M., Alswieleh, A. M., & Alyamani, B. J. (2018). Colorimetric aptasensor of vitamin D3: A novel approach to eliminate residual adhesion between aptamers and gold nanoparticles. *Scientific reports*, *8*(1), 1-12.

Bayat, P., Nosrati, R., Alibolandi, M., Rafatpanah, H., Abnous, K., Khedri, M., & Ramezani, M. (2018). SELEX methods on the road to protein targeting with nucleic acid aptamers. *Biochimie*, *154*, 132-155.

Berens, C., Groher, F., & Suess, B. (2015). RNA aptamers as genetic control devices: the potential of riboswitches as synthetic elements for regulating gene expression. *Biotechnology journal*, *10*(2), 246-257.

Bhardwaj, N., Bhardwaj, S. K., Nayak, M. K., Mehta, J., Kim, K.-H., & Deep, A. (2017). Fluorescent nanobiosensors for the targeted detection of foodborne bacteria. *TrAC Trends in Analytical Chemistry*, *97*, 120-135.

Castle, L. M., Schuh, D. A., Reynolds, E. E., & Furst, A. L. (2021). Electrochemical sensors to detect bacterial foodborne pathogens. *ACS sensors*, *6*(5), 1717-1730.

Chapman, P. A. (2000). Methods available for the detection of *Escherichia coli* O157 in clinical, food and environmental samples. *World Journal of Microbiology and Biotechnology*, *16*(8), 733-740.

Chase-Topping, M., Gally, D., Low, C., Matthews, L., & Woolhouse, M. (2008). Super-shedding and the link between human infection and livestock carriage of *Escherichia coli* O157. *Nature Reviews Microbiology*, *6*(12), 904-912.

Chekabab, S. M., Paquin-Veillette, J., Dozois, C. M., & Harel, J. (2013). The ecological habitat and transmission of *Escherichia coli* O157: H7. *FEMS microbiology letters*, *341*(1), 1-12.

Deisingh, A., & Thompson, M. (2004). Strategies for the detection of *Escherichia coli* O157: H7 in foods. *Journal of applied microbiology*, *96*(3), 419-429.

Evtugyn, G. (2016). Biosensor to Ensure Food Security and Environmental Control.

Gabriel, A. A., & Arellano, R. U. (2014). Decimal reduction times of acid-adapted and non-adapted *Escherichia coli* O157: H7, *Salmonella*

spp., and *Listeria monocytogenes* in young Cocos nucifera Linn. liquid endosperm. *Food Control*, *37*, 21-26.
Gayán, E., Geens, E., Berdejo, D., García-Gonzalo, D., Pagán, R., Aertsen, A., & Michiels, C. W. (2020). Combination of mild heat and plant essential oil constituents to inactivate resistant variants of *Escherichia coli* in buffer and in coconut water. *Food microbiology*, *87*, 103388.
Godambe, L. P., Bandekar, J., & Shashidhar, R. (2017). Species specific PCR based detection of *Escherichia coli* from Indian foods. *3 Biotech*, *7*(2), 1-5.
Hauser, E., & Lynn, J. (1940). Separation and fractionation of colloidal systems. *Industrial & Engineering Chemistry*, *32*(5), 659-662.
Holland, J., Louie, L., Simor, A., & Louie, M. (2000). PCR detection of *Escherichia coli* O157: H7 directly from stools: evaluation of commercial extraction methods for purifying fecal DNA. *Journal of clinical microbiology*, *38*(11), 4108-4113.
Hong, K. L., & Sooter, L. J. (2015). Single-stranded DNA aptamers against pathogens and toxins: Identification and biosensing applications. *BioMed research international*, *2015*.
Lee, E.-H., Lee, S. K., Kim, M. J., & Lee, S.-W. (2019). Simple and rapid detection of bisphenol A using a gold nanoparticle-based colorimetric aptasensor. *Food chemistry*, *287*, 205-213.
Liu, B., & Liu, J. (2017). Methods for preparing DNA-functionalized gold nanoparticles, a key reagent of bioanalytical chemistry. *Analytical methods*, *9*(18), 2633-2643.
Liu, B., & Liu, J. (2019). Interface-driven hybrid materials based on DNA-functionalized gold nanoparticles. *Matter*, *1*(4), 825-847.
Liu, Y.-M., Qiu, L., Sheng, A.-Z., Wan, X.-Y., Cheng, D.-Y., & Huang, J. (2018). Quantitative detection method of Enterocytozoon hepatopenaei using TaqMan probe real-time PCR. *Journal of invertebrate pathology*, *151*, 191-196.
Luan, Y., Chen, J., Xie, G., Li, C., Ping, H., Ma, Z., & Lu, A. (2015). Visual and microplate detection of aflatoxin B2 based on NaCl-induced aggregation of aptamer-modified gold nanoparticles. *Microchimica Acta*, *182*(5), 995-1001.
Matsunaga, K., Okuyama, Y., Hirano, R., Okabe, S., Takahashi, M., & Satoh, H. (2019). Development of a simple analytical method to determine arsenite using a DNA aptamer and gold nanoparticles. *Chemosphere*, *224*, 538-543.
Mondal, B., Ramlal, S., Lavu, P. S. R., Murali, H. S., & Batra, H. V. (2015). A combinatorial systematic evolution of ligands by exponential

enrichment method for selection of aptamer against protein targets. *Applied microbiology and biotechnology*, *99*(22), 9791-9803.
Moon, J., Kim, G., Park, S. B., Lim, J., & Mo, C. (2015). Comparison of whole-cell SELEX methods for the identification of *Staphylococcus aureus*-specific DNA aptamers. *Sensors*, *15*(4), 8884-8897.
Rotariu, L., Lagarde, F., Jaffrezic-Renault, N., & Bala, C. (2016). Electrochemical biosensors for fast detection of food contaminants–trends and perspective. *TrAC Trends in Analytical Chemistry*, *79*, 80-87.
Ruscito, A., & DeRosa, M. (2016). Small-Molecule Binding Aptamers: Selection Strategies, Characterization, and Applications. Front Chem. 2016; 4: 14. In.
Ruscito, A., Smith, M., Goudreau, D. N., & DeRosa, M. C. (2016). Current status and future prospects for aptamer-based mycotoxin detection. *Journal of AOAC International*, *99*(4), 865-877.
Saxena, T., Kaushik, P., & Mohan, M. K. (2015). Prevalence of *E. coli* O157: H7 in water sources: an overview on associated diseases, outbreaks and detection methods. *Diagnostic microbiology and infectious disease*, *82*(3), 249-264.
Scheiring, J., Andreoli, S. P., & Zimmerhackl, L. B. (2008). Treatment and outcome of Shiga-toxin-associated hemolytic uremic syndrome (HUS). *Pediatric nephrology*, *23*(10), 1749-1760.
Shih, C.-M., Chang, C.-L., Hsu, M.-Y., Lin, J.-Y., Kuan, C.-M., Wang, H.-K., Huang, C.-T., Chung, M.-C., Huang, K.-C., & Hsu, C.-E. (2015). based ELISA to rapidly detect *Escherichia coli*. *Talanta*, *145*, 2-5.
Szostak, J. W. (1992). In vitro genetics. *Trends in biochemical sciences*, *17*(3), 89-93.
Tabarzad, M., & Jafari, M. (2016). Trends in the design and development of specific aptamers against peptides and proteins. *The Protein Journal*, *35*(2), 81-99.
Templier, V., Roux, A., Roupioz, Y., & Livache, T. (2016). Ligands for label-free detection of whole bacteria on biosensors: A review. *TrAC Trends in Analytical Chemistry*, *79*, 71-79.
Yu, X., Chen, F., Wang, R., & Li, Y. (2018). Whole-bacterium SELEX of DNA aptamers for rapid detection of *E. coli* O157: H7 using a QCM sensor. *Journal of biotechnology*, *266*, 39-49.
Zhang, C., Yuan, Y., Zhang, S., Wang, Y., & Liu, Z. (2011). Biosensing platform based on fluorescence resonance energy transfer from upconverting nanocrystals to graphene oxide. *Angewandte Chemie International Edition*, *50*(30), 6851-6854.
Zhang, N., Qu, F., Luo, H. Q., & Li, N. B. (2013). Sensitive and selective

detection of biothiols based on target-induced agglomeration of silvernanoclusters. *Biosensors and Bioelectronics*, *42*, 214-218.

# 국문초록

이 연구에서 우리는 *E. coli* O157에 특이적인 압타머와 상보적 DNA 압타머가 결합된 AuNP의 응집에 기초하여 *E. coli* O157:H7의 현장에서 신속하며 민감하게 검출할 수 있는, 압타머가 결합된 이중 기능링커 AuNP를 이용한 비색 검출법을 개발하였다. 이 시스템에서 AuNP는 이중기능링커 및 응집보조 프로브로 사용되었으며, 각 AuNP 표면은 *E. coli* O157:H7 대상 압타머와 상보적인 DNA 서열의 압타머로 결합되었으며, 이는 각각 이중기능링커 AuNP (BL)와 응집보조 프로브 AuNP (AA)로 명명하였다. BL은 대상균이 존재하지 않을 때에는 상보적인 서열에 의해 AA와 결합하였으며, 양적균형에 의해 특정영역(REVC, 120 – 220 μL)에서 응집 및 침전이 일어났다. 하지만, 대상균이 투입되었을 때에는 경쟁적 결합 우선순위에 의해 상보적 서열의 AA가 아니라 대상균인 *E. coli* O157:H7과 결합하게 된다. 이는 기존의 양적균형에서의 차이를 일으키게 되고 대조군과 유사한 응집 및 침전이 일어나기 위해서는 기존보다 더 많은 양의 BL이 반응에 참여하여야 한다. 이를 통해 대조군과 대상균 간에는 REVC 영역의 변화가 발생하게 되며, 이를 통해 대상균의 유무를 확인할 수 있었다. 검출은 가장

민감하며 구분되는 BL 영역인 100, 120, 140 µL에서 진행되었으며, 최적화된 조건에서 $10^1$ ~ $10^6$ CFU/400 µL의 검출 범위와 57 ± 0.5 CFU/400 L의 검출 한계를 나타냈다. 또한 압타머 기반의 BL을 이용한 비색분석법은 실제 매트릭스인 코코넛워터에서도 on/off 감지 시스템으로 매우 우수하게 평가되었다. 따라서 제안된 압타머 기반의 BL을 이용한 비색분석법은 식중독을 일으키는 병원체를 현장에서 검출하는 데 적합한 방법이 될 수 있을 것으로 기대된다. 또한, 본 연구를 통해 실제 매트릭스에서 병원균 분석을 위한 앱타머 기반 비색 분석 개발에 대한 향후 연구의 기반을 제공할 수 있었다. 이 압타머 기반 비색 분석법은 A) 압타머 서열과 표적 사이의 친화성, B) 압타머와 그 상보적인 DNA 압타머 사이의 친화력이라는 두 가지 경쟁적인 상호 작용 역학에 의해 구동되었다.

**주요어:** 비색검출법, 압타머, 이중기능링커, 응집보조, *E. coli* O157:H7, 실제 식품

학번: 2021-20519